Enzyme Catalysis and Regulation:

Replacement of a Phenylalanine by a Tyrosine in the Active Site Confers Fructose-6-phosphate Aldolase Activity to the Transaldolase of *Escherichia coli* and Human Origin

Sarah Schneider, Tatyana Sandalova, Gunter Schneider, Georg A. Sprenger and Anne K. Samland

J. Biol. Chem. 2008, 283:30064-30072.
doi: 10.1074/jbc.M803184200 originally published online August 7, 2008

THE JOURNAL OF BIOLOGICAL CHEMISTRY VOL. 283, NO. 44, pp. 30064–30072, October 31, 2008

Replacement of a Phenylalanine by a Tyrosine in the Active Site Confers Fructose-6-phosphate Aldolase Activity to the Transaldolase of *Escherichia coli* and Human Origin*[S]

Received for publication, April 25, 2008, and in revised form, June 18, 2008 Published, JBC Papers in Press, August 7, 2008, DOI 10.1074/jbc.M803184200

Sarah Schneider[‡], Tatyana Sandalova[§], Gunter Schneider[§], Georg A. Sprenger[‡], and Anne K. Samland[‡1]

From the [‡]Institute of Microbiology, Universität Stuttgart, 70550 Stuttgart, Germany and the [§]Division of Molecular Structural Biology, Department of Medical Biochemistry and Biophysics, Karolinska Institutet, 17177 Stockholm, Sweden

Based on a structure-assisted sequence alignment we designed 11 focused libraries at residues in the active site of transaldolase B from *Escherichia coli* and screened them for their ability to synthesize fructose 6-phosphate from dihydroxyacetone and glyceraldehyde 3-phosphate using a newly developed color assay. We found one positive variant exhibiting a replacement of Phe[178] to Tyr. This mutant variant is able not only to transfer a dihydroxyacetone moiety from a ketose donor, fructose 6-phosphate, onto an aldehyde acceptor, erythrose 4-phosphate (14 units/mg), but to use it as a substrate directly in an aldolase reaction (7 units/mg). With a single amino acid replacement the fructose-6-phosphate aldolase activity was increased considerably (>70-fold compared with wild-type). Structural studies of the wild-type and mutant protein suggest that this is due to a different H-bond pattern in the active site leading to a destabilization of the Schiff base intermediate. Furthermore, we show that a homologous replacement has a similar effect in the human transaldolase Taldo1 (aldolase activity, 14 units/mg). We also demonstrate that both enzymes TalB and Taldo1 are recognized by the same polyclonal antibody.

Transaldolase (Tal)[2] is a ubiquitous enzyme that is present in all domains of life. It is part of the non-oxidative path of the pentose phosphate pathway. Here, it catalyzes the reversible transfer of a dihydroxyacetone (DHA) moiety from a ketose donor, *e.g.* fructose 6-phosphate (Fru-6-P), onto an aldehyde acceptor, *e.g.* erythrose 4-phosphate (Ery-4-P). The best studied example is transaldolase B (TalB) from *Escherichia coli* (1). A number of structural and mechanistic studies have been published elucidating its reaction mechanism (1–6). Similar to class I aldolases the reaction proceeds via a Schiff base intermediate. TalB is a homo-dimer and the monomer exhibits a $(\beta/\alpha)_8$-barrel fold where the C-terminal helix lies across the barrel opening at one site (5). A similar structure had been determined for the human transaldolase (7).

Recently, a fructose-6-phosphate aldolase (FSA) of *E. coli* has been discovered by our group (8) that uses DHA as donor substrate and catalyzes the reversible formation of Fru-6-P from DHA and GAP (Fig. 1). Multiple sequence alignments of different Tal sequences demonstrate that FSA resides within the family of transaldolases (8, 9) and does show little similarity to DHAP-dependent aldolases, such as class I fructose-1,6-bisphosphate aldolase. Also the FSA monomer is highly similar to TalB exhibiting a similar $(\beta/\alpha)_8$-barrel fold (9). But in contrast to TalB, FSA forms a homo-decamer, which is arranged by two doughnut-shaped pentameric rings where the C-terminal helix of one subunit interacts with the adjacent subunit (9). With 220 amino acids compared with 317 amino acids FSA is smaller than TalB and shows about 20% sequence identity to TalB. Mechanistically, it is a class I aldolase, *i.e.* the reaction proceeds via a Schiff base intermediate.

In this study, we addressed the differences between Tal and FSA concerning their enzymatic features especially the Fru-6-P cleavage. Therefore, we compared TalB and FSA from *E. coli* using a structure-assisted sequence alignment (Fig. 2) to identify differences in sequence in or close to the active site of TalB. We chose 11 positions at which site-saturation mutagenesis libraries were created. Screening of these libraries for Fru-6-P formation from DHA and GAP was performed using a newly developed color assay. One replacement, Phe[178] to Tyr, resulted in a strongly elevated FSA activity and we here report a detailed functional and structural characterization of the human and *E. coli* Tal F189Y and F178Y variants, respectively. The described muteins are examples of a change in enzyme class from a transferase to a lyase conferred by a single amino acid replacement.

EXPERIMENTAL PROCEDURES

Chemicals and Auxiliary Enzymes—Antibiotics, acrylamide-bisacrylamide, sugars, buffer components, and culture media for bacteria were from Carl Roth GmbH (Karlsruhe, Germany). Restriction enzymes were purchased from New England Biolabs (Frankfurt, Germany) and MBI fermentas (St. Leon-Rot, Germany). Sugar phosphates and aldehydes were from Sigma/Fluka (Taufkirchen, Germany). Auxiliary enzymes were from

* This work was supported by Deutsche Forschungsgemeinschaft Grant SPP1170/Sp503/4-2 (to G. Sprenger) and a grant from the Swedish Research Council (to G. Schneider). The costs of publication of this article were defrayed in part by the payment of page charges. This article must therefore be hereby marked "*advertisement*" in accordance with 18 U.S.C. Section 1734 solely to indicate this fact.

[S] The on-line version of this article (available at http://www.jbc.org) contains supplemental Tables S1 and S2 and Figs. S1 and S2.

The atomic coordinates and structure factors (code 3CWN) have been deposited in the Protein Data Bank, Research Collaboratory for Structural Bioinformatics, Rutgers University, New Brunswick, NJ (http://www.rcsb.org/).

[1] To whom correspondence should be addressed: Allmandring 31, D-70550 Stuttgart, Germany. Tel.: 49-711-6856-5491; Fax: 49-711-6856-5725; E-mail: anne.samland@imb.uni-stuttgart.de.

[2] The abbreviations used are: Tal, transaldolase; DHA, dihydroxyacetone; Ery-4-P, D-erythrose 4-phosphate; Fru-6-P, D-fructose 6-phosphate; FSA, fructose-6-phosphate aldolase; GAP, DL-glyceraldehyde 3-phosphate; GST, glutathione *S*-transferase; hTal, human transaldolase (Taldol).

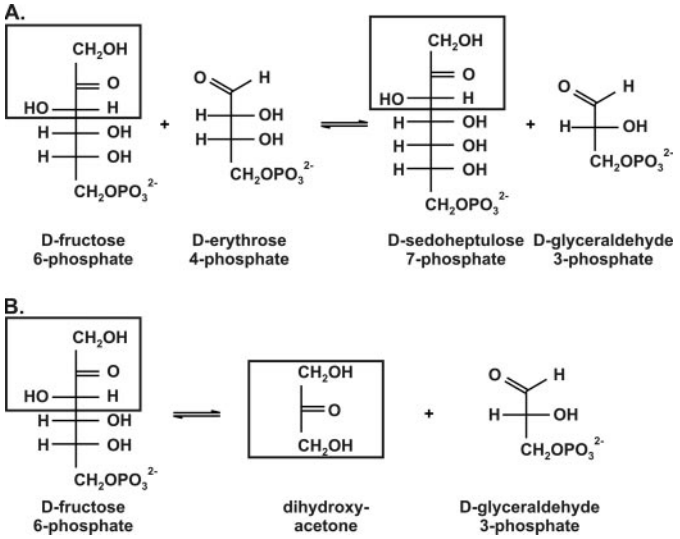

FIGURE 1. *A*, transaldolase B of *E. coli* cleaves fructose 6-phosphate (donor) and transfers a dihydroxyacetone moiety onto erythrose 4-phosphate (acceptor). In this reaction sedoheptulose 7-phosphate and glyceraldehyde 3-phosphate are produced. *B*, fructose-6-phosphate aldolase of *E. coli* cleaves fructose 6-phosphate into dihydroxyacetone and glyceraldehyde 3-phosphate.

Roche Applied Science (Mannheim, Germany). Q-Sepharose and gel filtration matrix Superdex 200pg were from Amersham Biosciences/GE Healthcare, histidine-tagged affinity column matrix nickel-nitrilotriacetic acid was purchased from Qiagen (Hilden, Germany).

Strains and Plasmids—Bacterial strains, plasmids, and oligonucleotides used in this study are listed in supplementary data Tables S1 and S2.

Site-directed Saturation Mutagenesis—The *talB* gene was amplified by PCR from chromosomal DNA of *E. coli* W3110 and cloned into the pET28a vector. During this amplification 4 bases at positions 726 (G–T), 738 (G–T), 739 (G–A), and 759 (G–T) were changed as compared with the sequence in the data base (10). This results inadvertently in an amino acid replacement of Ala by Thr at position 247. The NdeI-XhoI fragment of pET28*talB* was cloned into expression vector pJF119EH (11). This fragment contained the ribosomal binding site of the pET28a vector, an N-terminal His_6 tag, and the *talB* gene of *E. coli* W3110. Site-directed saturation mutagenesis was performed using the QuikChange® II Site-directed Mutagenesis Kit from Stratagene (Amsterdam, The Netherlands) and degenerated oligonucleotides (biomers, Ulm, Germany) with NNS degeneracy (N, A/C/G/T; S, C/G). Thereby, 32 codons and all 20 proteinogenic amino acid residues were obtained. The libraries were transformed into XL1Blue cells (Stratagene). The plasmid DNA of 30 randomly picked clones of one library (Phe178X) were isolated with the NucleoSpin Kit II (Macherey + Nagel, Düren, Germany) and custom sequenced by MWG Biotech AG (Martinsried, Germany). For 10 randomly picked clones the expression in crude extracts was checked via SDS-PAGE. All of them expressed the corresponding His_6-TalBF178X variant protein in considerable amounts.

Cultivation and Protein Expression in Deepwell Plates—Single colonies were randomly picked and arrayed in 96-deepwell plates (volume 2 ml; Greiner Bio-One, Frickenhausen, Germany). Each well contained 1 ml of 2YT broth (12) with 100 μg/ml ampicillin. The plate was sealed with a gas-permeable adhesive film and incubated at 37 °C with shaking at 145 rpm overnight. These cultures were used to inoculate expression cultures (1:20) containing 1 ml of 2YT broth supplemented with 100 μg/ml ampicillin and 1 mM (final concentration) isopropyl β-D-thiogalactopyranoside. These expression cultures were grown at 37 °C with shaking at 145 rpm overnight. The cells were collected by centrifugation (1600 × *g* at 8 °C for 10 min), supernatants were discarded. Cell pellets were resuspended in 100 μl of 50 mM glycylglycine buffer (pH 8.5) containing 1 mg/ml lysozyme (Roche) and 0.1 mg/ml DNase I (Roth). Cell debris was collected by centrifugation (1600 × *g* at 8 °C for 10 min) and 100 μl of the cell-free extracts were transferred to a new 96-well microtiter plate for enzyme assay.

Color Assay for FSA Activity—The previously described assay for fructose 6-phosphate formation (8) was adapted for screening in a microtiter plate format. The formation of Fru-6-P was coupled to the reduction of $NADP^+$ via phosphoglucose isomerase and glucose-6-phosphate dehydrogenase. NADPH was visualized by the formation of a lilac formazan complex. This allowed a visual detection of the appearance of positive hits. For quantitative analysis the increase in color was monitored for 20 min at 540 nm at 25 °C using a multiwell photometer (Spectra Max Plus, Molecular Devices, Ismaning/Munich, Germany).

The assay contained 50 mM glycylglycine buffer (pH 8.5), DHA (50 mM), DL-glyceraldehyde 3-phosphate (GAP, 2.8 mM), $NADP^+$ (0.5 mM), phosphoglucose isomerase (0.1 unit), glucose-6-phosphate dehydrogenase (0.1 unit), nitro tetrazolium blue chloride (0.5 mM), and diaphorase (0.3 milliunit, Sigma). The reaction was started by adding cell-free extract (≤5 μg of protein). Protein concentrations were measured in microtiter plates using a dye-binding method (13). The activities were monitored as an increase in OD_{540} per min and standardized over the protein concentration using Microsoft Excel XP (Unterschleißheim, Germany). Cell-free extracts containing FSA and His_6-TalBwt were used as positive and negative controls, respectively. The standard deviations of the activities of the positive and negative controls were <20%.

Protein Purification of His_6-TalBwt and His_6-TalBF178Y—From cell-free extracts of the *E. coli* XL1Blue recombinant strains (XL1Blue-pJF119*talB* and XL1Blue-pJF119*talBF178Y*), His_6-TalB and His_6-TalBF178Y were purified by nickel-nitrilotriacetic acid affinity chromatography as recommended by the supplier (Qiagen, The QIAexpressionist™, 5th edition). Fractions containing transaldolase activity were pooled and the buffer was changed to 50 mM glycylglycine (pH 8.5) containing 1 mM dithiothreitol using a concentrator unit (Vivaspin MWC 10,000 Da; Vivascience, Göttingen, Germany). The purity was estimated by SDS-PAGE (14).

Purification of FSA—From cell-free extracts of recombinant strain BL21(DE3) *Star pLysS*-pET16*fsa*, FSA was purified as described previously (15). After heat treatment (20 min, 75 °C) and centrifugation (100,000 × *g* at 4 °C for 35 min) the supernatant was applied to an anion exchange column (Q-Sepharose HP (16/10)). The FSA activity containing fractions were pooled and buffer was exchanged to 50 mM glycylglycine buffer (pH 8.0) containing 1 mM dithiothreitol. The protein purity was determined by SDS-PAGE and estimated to ≥98% purity.

Activity Assays—All enzyme assays were performed in 50 mM glycylglycine buffer (pH 8.5) containing 1 mM dithiothreitol at 30 °C. Using a Cary 100 Bio UV-Visible Spectrophotometer (Varian, Darmstadt, Germany) the enzyme activity was monitored at 340 nm for 10 min.

For the transaldolase reaction D-fructose 6-phosphate (10 mM) and D-erythrose 4-phosphate (2 mM according to 61% purity of the supplied material) were used as substrates. The formation of GAP was detected via the formation of NAD^+ from NADH using the coupling enzymes triose-phosphate isomerase and glycerol-3-phosphate dehydrogenase. The assay was performed as described (1, 16). To distinguish between the Fru-6-P cleavage activity and Tal activity the reaction was started with Ery-4-P. The decrease of NADH in the presence of Fru-6-P was subtracted from the decrease in the presence of both substrates, Fru-6-P and Ery-4-P. For determination of the K_m value for D-fructose 6-phosphate a concentration range of 1 to 50 mM (His_6-TalBwt), 1 to 150 mM (His_6-TalBF178Y), and 0.5 to 60 mM (hTalwt, hTalF89Y) were used at a constant concentration of D-erythrose 4-phosphate (2 mM). This concentration of D-erythrose 4-phosphate is saturating as the K_m value for TalB is 90 μM (1). The specific activity was plotted against the Fru-6-P concentration. The hyperbolic function of the Michaelis-Menten equation was fitted to the data using SigmaPlot 9.0 (Systat Software, Erkrath, Germany).

The cleavage of D-fructose 6-phosphate into dihydroxyacetone and D-glyceraldehyde 3-phosphate was monitored via an enzyme coupled assay as described previously (8). Again, the formation of GAP is detected. The K_m value for D-fructose 6-phosphate was determined using concentrations of D-fructose 6-phosphate ranging from 1 to 50 mM (FSAwt), 1 to 20 mM (His_6-TalBF178Y), or 0.25 to 60 mM (hTalF189Y).

The formation of D-fructose 6-phosphate from dihydroxyacetone and DL-glyceraldehyde 3-phosphate was determined as described previously (8) via the coupling enzymes phosphoglucose isomerase and glucose-6-phosphate dehydrogenase. The K_m value for dihydroxyacetone was determined using 10 to 300 mM (FSAwt), 10 to 350 mM (His_6-TalBF178Y), or 10 to 600 mM (hTalF189Y). The concentration of DL-glyceraldehyde 3-phosphate was kept constant at 2.8 mM. This concentration of DL-glyceraldehyde 3-phosphate was saturating as the K_m value for TalB was 38 μM (1).

Gel Filtration—The molecular mass of His_6-TalBF178Y and hTalF189Y under native conditions was determined by size exclusion chromatography. Gel filtration was performed on a Superdex 200pg (10/30) column and a fast protein liquid chromatography system (Amersham Biosciences). The column was equilibrated with 50 mM glycylglycine buffer (pH 8.5) containing 150 mM sodium chloride and 1 mM dithiothreitol with a flow rate of 0.5 ml/min at 4 °C. The column was calibrated with reference proteins of known molecular masses between 13.7 and 440 kDa (ribonuclease A, 13.7 kDa; chymotrypsinogen A, 25 kDa; ovalbumin, 43 kDa; albumin, 67 kDa; aldolase, 158 kDa; catalase, 232 kDa; ferritin, 440 kDa; purchased from GE Healthcare). The void volume was determined with blue dextran 1000.

Crystallization and Structure Determination—Crystals of the *E. coli* TalB mutant F178Y were obtained at room temperature by the hanging-drop vapor diffusion method at several conditions, all conditions contained polyethylene glycol and different salts. The best diffracting crystals were obtained in 18% polyethylene glycol 3350, 0.2 M ammonium sulfate, without addition of any buffer. Two μl of a 60 mg/ml protein solution in 50 mM glycylglycine (pH 8) were mixed with 4 μl of the crystallization reservoir solution and equilibrated against 1 ml of mother liquor. Crystals grew during several days to a size of 0.2 × 0.1 × 0.05 mm. X-ray data were collected at beamline ID14-3 (ESRF Grenoble, France) (λ = 0.931 Å) using an ADSC Q4 CCD detector. The crystals were soaked for several seconds in crystallization solution containing 25% glycerol before freezing in a stream of liquid nitrogen. Crystals of the F178Y mutant belong to the same orthorhombic space group $P2_12_12_1$ as wild-type protein with slightly different cell dimensions a = 65.9 Å, b = 86.2 Å, c = 131.2 Å. All diffraction data were processed with the program MOSFLM, scaled, and merged with SCALA from the CCP4 suite of programs (17). The data collection statistics are given in Table 1.

TABLE 1
Data collection and refinement statistics

Data collection	
Space group	$P2_12_12_1$
Unit cell (Å)	a = 65.9, b = 86.2, c = 131.2
Resolution (Å)	47-1.4 (1.48-1.4)
No. of unique reflections	135,268 (13,203)
R_{merge}	0.037 (0.15)
Redundancy	3.7 (2.4)
Mean $I/\sigma(I)$	21.4 (5.7)
Completeness	92.0% (62%)
Refinement	
R/R_{free}	14.9/17.3
No. of protein atoms	5,116
No. of ions	4
No. of water molecules	605
Root mean square deviation bonds (Å)	0.09
Root mean square deviation angles (°)	1.2
Average *B*-factor (Å)²	
Protein	11.8
Ions	15.5
Water	21.7
Ramachandran plot	
Most favoured (%)	98.2
Allowed	1.6
Outliers	0.2

The structure of the F178Y mutant was solved by molecular replacement with MOLREP (18) using a subunit of wild-type *E. coli* TalB (5) (Protein Data Bank 1ONR) as a template. Estimation of the solvent content in the crystals of F178Y suggested that the asymmetric unit contains two subunits. The native Patterson map shows a strong peak (50% of the origin peak) at 0.0, 0.5, and 0.076 indicating the presence of translational symmetry. The best solution found with MOLREP had an *R*-factor of 0.434 and a score of 0.75. Refinement of the model using REFMAC5 (19) was monitored by R_{free} and alternated with manual inspection and rebuilding in *COOT* (20). The final model contains 631 amino acid residues (residues 2–317 for chain A and 3–317 for chain B), 4 sulfate ions, and 717 water molecules. Refinement statistics are shown in Table 1. The crystallographic data for the F178Y mutant has been deposited with the Protein Data Bank accession code 3CWN.

Cloning and Mutagenesis of the Human taldo1 Gene—The full-length cDNA clone IRATp970D0610D was obtained from the RZPD data base (Deutsches Ressourcenzentrum für

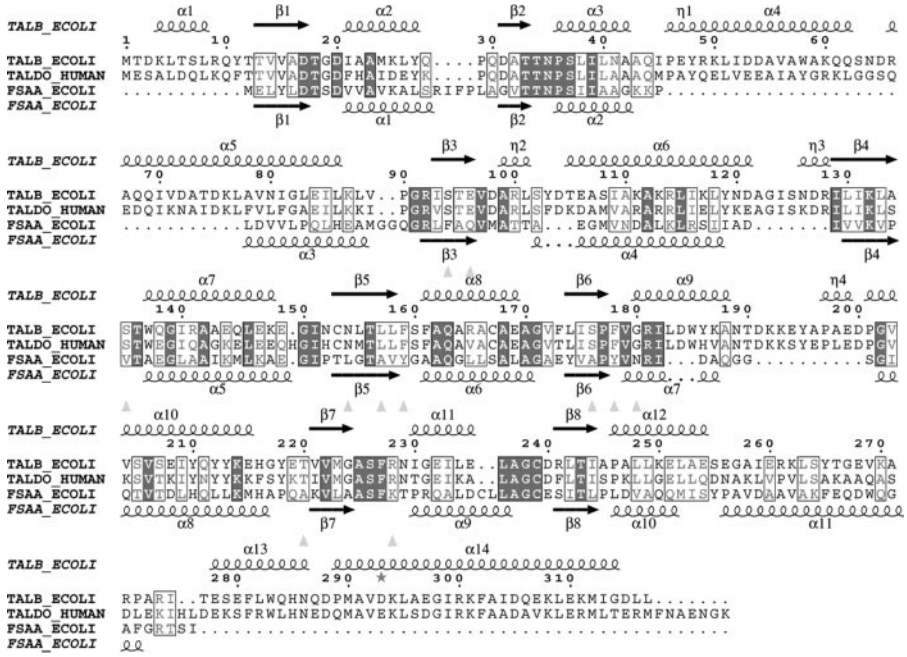

FIGURE 2. **Structure-based sequence alignment of TalBwt and FSAwt from *E. coli* and hTal from *Homo sapiens sapiens*.** *Above* and *below* the sequence alignment the secondary structural elements of TalBwt (5) and FSA (9), respectively, are shown. A *gray background* indicates invariant residues, and *residues labeled in gray* are highly conserved. Positions selected for saturation mutagenesis are highlighted by *gray triangles*.

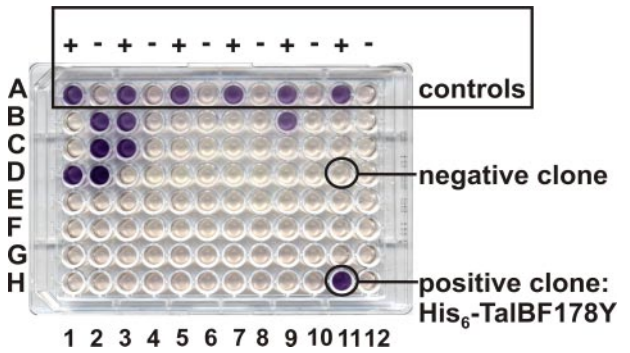

FIGURE 3. **Color assay of 84 randomly picked clones of the TalBPhe178X library.** The formation of fructose 6-phosphate from dihydroxyacetone and glyceraldehyde 3-phosphate is detected with an enzyme coupled color assay. In this assay fructose 6-phosphate is isomerized into glucose 6-phosphate (phosphoglucose isomerase), which is then oxidized to 6-phosphogluconolactone (glucose-6-phosphate dehydrogenase) under concomitant consumption of NADPH. In a third step, using diaphorase, $NADP^+$ is reduced again and nitro blue tetrazolium is oxidized to a *lilac* formazan complex. The controls are shown in the first row and in the rows below are the randomly picked clones. Positive clones display a *dark lilac* color (D1, B-D2, B/D3, B9, H11; all these clones possess the same amino acid exchange: Phe to Tyr) whereas all the others are negative clones with a *pale yellow* color.

Genomforschung GmbH, Berlin, Germany). The coding sequence for the human transaldolase Taldo1 (hTal) (21) was amplified by PCR and cloned into expression vector pGEXTN* using restriction sites NdeI and SmaI. This allows the co-transcription and translation as GST fusion protein. The coding sequence was verified by sequencing. However, a comparison with the taldo1 sequence (21) revealed a deletion of 4 bases at position 829 bp resulting in a frameshift. Site-directed mutagenesis for correction of this deletion and replacement of Phe^{189} by Tyr was carried out using a modified version of the QuikChange® protocol. In this case the ReproFast Polymerase from GENAXXON (Biberach, Germany) was used. The correct sequence was confirmed by custom sequencing (MWG Biotech AG).

Heterologous Expression and Purification of Human Tal—GST-hTal and GST-hTalF189Y were expressed in an *E. coli* LJ110 (DE3) $talA^-talB^-$ pLysSRARE recombinant strain (LJ110-pGEXTN**htal* and LJ110-pGEXTN**htalF189Y*). This strain containing the DE3 system (22) was deficient in both genes encoding for transaldolase, *talA* and *talB*,[3] and carried the pLysSRARE2 plasmid (23). The chromosomal deletion of *talA* and *talB* was performed by the method described by Datsenko and Wanner (24) in the *E. coli* strain BW25113. Using P1 phage transduction (12) it was transferred to *E. coli* LJ110 (DE3) strain. hTal and hTalF189Y were purified by a glutathione-Sepharose column as recommended by the supplier (GE Healthcare). The GST tag was cleaved off using TEV-Protease (25) in an on-column digest overnight. The buffer was changed to 50 mM glycylglycine (pH 8.5) containing 1 mM dithiothreitol using a concentrator unit (Vivaspin MWC 10,000 Da; Vivascience, Göttingen, Germany).

Immunodetection—5- and 15-μg cell-free extracts expressing TalB or GST-hTal variants, respectively, were separated by 12% (v/v) SDS-PAGE and stained with Coomassie Brilliant Blue. A second gel was run in parallel with 5 and 20 μg of cell-free extract and the proteins were transferred to a polyvinylidene fluoride membrane for immunodetection (Roche). Western blotting was done by standard procedures. The blotted transaldolase proteins were decorated with a polyclonal antibody against TalB from guinea pig (4). Anti-guinea pig antibody coupled to alkaline phosphatase (Sigma) was used as second antibody and color development with nitro blue tetrazolium chloride and 5-bromo-4-chloro-3-indolyl-phosphate *p*-toluidine salt was monitored. Prestained all blue SDS-PAGE standard proteins (Bio-Rad) were used as marker proteins.

RESULTS

Generation and Screening of Mutant Libraries—Based on a structure-assisted sequence alignment (Fig. 2) 11 positions were identified in or close to the active site of FSA and TalB from *E. coli*. At these positions both enzymes differ in their primary sequence. We reasoned that by changing these residues it was possible to confer an aldolase activity upon TalB. Therefore, at the following positions a site-saturation library was generated using *talB* as template: Ser^{94}, Glu^{96}, Ser^{135}, Asn^{154}, Leu^{157}, Phe^{159}, Ser^{176}, Phe^{178}, Gly^{180}, Thr^{220}, and Arg^{228}. By applying a newly developed color assay (Fig. 3) it was

[3] A. K. Samland and G. A. Sprenger, unpublished results.

TABLE 2

Kinetics for His_6-TalBF178Y from *E. coli*, and hTalF189Y from *H. sapiens sapiens* as well as FSA from *E. coli* for the formation and cleavage of D-fructose 6-phosphate

Protein		His_6-TalBwt	His_6-TalBF178Y	FSA	hTalwt	hTalF189Y
Reaction						
Fru-6-P synthesis from DHA and GAP	V_{max} (units/mg)	ND[a]	7 ± 1[b]	20 ± 1[b]	N.detect.[c]	14[d]
	k_{cat}[e] (s^{-1})	ND	4.3 ± 0.7[b]	7.6 ± 0.5	N.detect.	8.9[d]
	K_m (DHA) (mM)	ND	30 ± 4[b]	62 ± 7[b]	N.detect.	340[d]
	k_{cat}/K_m (M^{-1} s^{-1})	ND	150 ± 30	130 ± 8	N.detect.	26
Fru-6-P cleavage into DHA and GAP	V_{max} (units/mg)	N.detect.	0.36 ± 0.05[b]	3.4 ± 0.7[b]	N.detect.	0.32 ± 0.04[f]
	k_{cat}[e] (s^{-1})	N.detect.	0.22 ± 0.03[b]	1.3 ± 0.3	N.detect.	0.21 ± 0.02[f]
	K_m (F6P) (mM)	N.detect.	1.5 ± 0.2[b]	12 ± 3[b]	N.detect.	0.76 ± 0.11[f]
	k_{cat}/K_m (M^{-1} s^{-1})	N.detect.	150 ± 26	130 ± 35	N.detect.	270 ± 11

[a] ND, not determined; activity ≤0.1 unit/mg using 50 mM DHA and 2.8 mM DL-GAP.
[b] Average value from four independent measurements.
[c] N. detect., not detectable; activity <0.01 units/mg.
[d] Average value from two independent measurements (deviation ≤14%).
[e] k_{cat} was calculated as turnover number per active sites, *i.e.* monomeric subunits.
[f] Average value from three independent measurements.

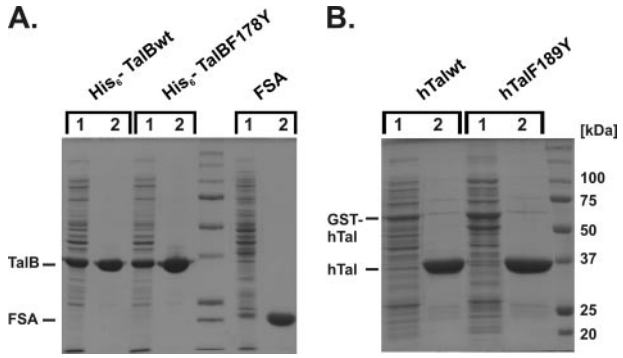

FIGURE 4. *A*, SDS-PAGE analysis of His_6-TalBwt, His_6-TalBF178Y, and FSAwt. *B*, SDS-PAGE analysis of hTalwt and hTalF189Y. Cell-free extracts (10 μg/protein each, *lane 1*) and purified proteins (10 μg/protein each, *lane 2*) were applied to a 12% (v/v) SDS-PAGE. Protein bands were visualized by staining with Coomassie Brilliant Blue R-250. Using a precious protein standard prestained from Bio-Rad the molecular mass of the enzymes were verified (FSA, 24 kDa; His_6-TalBwt and His_6-TalBF178Y, 37 kDa; GST-hTalwt and GST-hTalF189Y, 65 kDa; hTalwt and hTalF189Y, 37.5 kDa, enzyme masses are calculated using ExPASY).

possible to screen hundreds of clones in microtiter plates for the formation of Fru-6-P from DHA and GAP as substrate. DHA is a very poor substrate for TalBwt (Table 2).

In a first round one plate of each focused library was screened, corresponding to 84 clones. Only the focused library at position Phe^{178} contained active clones. To ensure that all possible 20 amino acid replacements were covered a total of 252 clones were screened for the focused library Phe178X. Clones exhibiting an activity at least twice as high as the background (negative control, His_6-TalBwt) were re-cultivated and re-screened in deepwell plates. Of 252 clones 19 exhibiting consistently FSA activity were sequenced. All of them possessed a TAC triplet instead of TTT coding for Tyr instead of Phe. No additional mutations had occurred. These results demonstrate that of the 11 positions chosen for the generation of focused libraries only position Phe^{178} is critical for gain of a fructose-6-phosphate aldolase activity. Furthermore, nature selected in FSA the best and only possible amino acid residue for conferring this activity.

Purification and Quaternary Structure of the His_6-TalBF178Y Mutein—To characterize the TalBF178Y variant in more detail the mutant protein (mutein) was purified to an estimated purity of 97% (Fig. 4). From 1 g wet *E. coli* cells about 10 and 9 mg of His_6-TalBwt and His_6-TalBF178Y mutein, respectively, were recovered.

FSA and TalB exhibit a similar subunit structure of a $(\beta/\alpha)_8$-barrel fold but differ in their quarternary structure. FSA is a homo-decamer (9), whereas TalB is a homo-dimer (5). Furthermore, it had been shown that the dimeric structure of TalB can be disrupted by a single mutation into active monomers (3). Therefore, we used size exclusion chromatography to determine the native mass of the His_6-TalBF178Y mutein. The size of the monomer was calculated to 37 kDa using EXPASY (www.expasy.org/tools/pi_tool.html). The His_6-TalBF178Y mutein behaves similar to His_6-TalB on a Superdex 200pg (10/30) column corresponding to a mass of 75 ± 10 kDa (data not shown). This indicates that neither the mutation nor the His tag interferes with the dimeric structure of TalB.

Mutagenesis and Purification of the Human TalF189Y Mutein—To check whether the altered activity conferred by the replacement is transferable to other related transaldolases we cloned the hTal as a GST fusion protein from a cDNA clone and exchanged the phenylalanine at the respective position (Phe^{189} in Taldo1) to a tyrosine. The mutant variant and the wild-type enzyme were purified by affinity chromatography (Fig. 4). The yield of the purified enzymes was 1 order of magnitude lower than compared with the *E. coli* transaldolase: 0.5 mg for the wild-type enzyme and 0.9 mg for the hTalF189Y mutein from 1 g wet *E. coli* cells. The purity was similar with 97%.

The native mass was determined by size exclusion chromatography. Both proteins, hTal and hTalF189Y, migrated similarly on a Superdex 200pg (10/30) column (data not shown). Hence, they form a dimer of 77 ± 10 kDa (calculated size of monomer 37.5 kDa). The high similarity between the human and the *E. coli* transaldolase was confirmed by the fact that a polyclonal antibody raised against TalB (4) detects the human transaldolase in an immunoblot (Fig. 5).

FSA and Tal Activity of the His_6-TalBF178Y and hTalF189Y Muteins—The purified enzymes were used to determine the kinetic constants of the FSA and Tal reactions (Tables 2 and 3 and supplementary data Fig. S1). For the formation of Fru-6-P, the reaction that had been used for screening the His_6-TalBF178Y mutein exhibits a considerable activity with a V_{max}

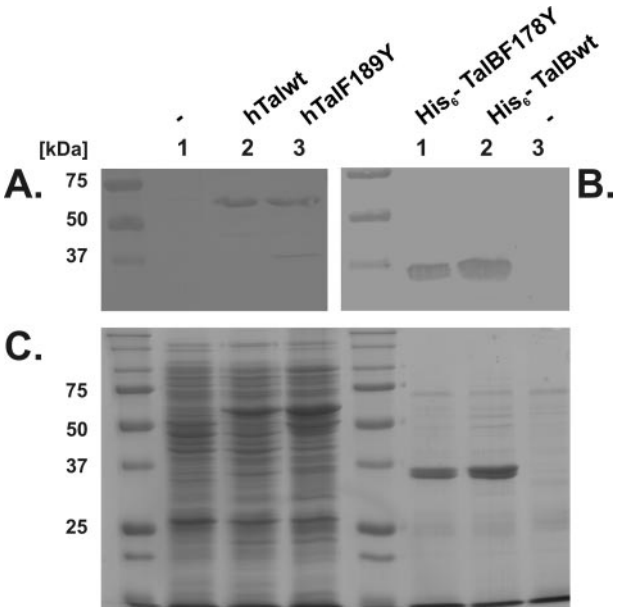

FIGURE 5. **Immunodetection (*A* and *B*) and SDS-PAGE analysis (*C*) of cell-free extracts containing His_6-TalBwt, His_6-TalBF178Y, GST-hTalwt, and GST-hTalF189Y.** The crude extracts (5 μg/protein for TalB variants and 15 μg/protein for hTal variants) were separated on 12% (v/v) SDS-PAGE. Proteins were stained with Coomassie Brilliant Blue R-250 (*C*) or blotted on a polyvinylidene fluoride membrane and immunodetection with a polyclonal antibody against TalB was performed (*A* and *B*).

of 7 ± 1 units/mg, whereas His_6-TalB has a lower activity of ≤0.1 units/mg (using 50 mM DHA and 2.8 mM DL-GAP). FSA shows a V_{max} of 20 ± 1 unit/mg. The K_m value of the His_6-TalBF178Y mutein for DHA is 30 ± 4 mM 2-fold lower than the K_m value of FSA (62 ± 7 mM). Therefore, both enzymes exhibit a similar catalytic efficiency (k_{cat}/K_m) for Fru-6-P synthesis (150 and 130 M^{-1} s^{-1}, respectively). As Fru-6-P was detected enzymatically it is confirmed that this stereoisomer is formed. However, it cannot be excluded completely that other isomers are formed as well. According to NMR measurements, the His_6-TalBF178Y mutein exhibits a similar enantiospecificity of ≥90% as FSA.[4] For hTal wild-type no activity was measured in the reaction (<0.01 units/mg). On the other hand, the hTalF189Y mutein exhibits a V_{max} of 14 units/mg similar to the *E. coli* mutein. But the K_m value for DHA (340 mM) is considerably higher than for TalBF178Y and FSA. Hence, the catalytic efficiency (26 M^{-1} s^{-1}) is about 5-fold lower than for FSA and TalBF178Y.

In the reverse reaction, the cleavage of Fru-6-P, the formation of GAP was monitored in an enzyme coupled assay. For the retroaldol reaction V_{max} is lower with 0.36 ± 0.05 units/mg for the His_6-TalBF178Y mutein, 0.32 ± 0.04 units/mg for the hTalF189Y mutein, and 3.4 ± 0.7 units/mg for FSA. The wild-type enzymes (His_6-TalB and hTal) do not show any activity with Fru-6-P as the sole substrate (<0.01 units/mg). As a transferase they strictly require an acceptor substrate. For all DHAP- and DHA-dependent aldolases the direction of synthesis is preferred (8, 26). The K_m values for Fru-6-P were determined to 1.5 ± 0.2 mM for the His_6-TalBF178Y mutein and 0.76 ± 0.11 mM for the hTalF189Y mutein. The K_m value for Fru-6-P of FSA is higher with 12 ± 3 mM.

With a new activity present, we wondered whether Tal activity was retained. For Tal activity the standard reaction using Fru-6-P and Ery-4-P as substrates was monitored. Again the formation of GAP was measured in an enzyme coupled assay. Compared with His_6-TalB (85 ± 9 units/mg) the His_6-TalBF178Y mutein shows a reduced V_{max} of 14 ± 1 units/mg and an elevated K_m value of 22 ± 5 mM (His_6-TalB 3.0 ± 0.2 mM). This leads to a more than 30-fold reduction in catalytic efficiency (His_6-TalB, 18,000 M^{-1} s^{-1}; His_6-TalBF178Y, 530 M^{-1} s^{-1}). For the His_6-TalBF178Y mutein the catalytic efficiency for the Tal activity is still higher than for the FSA activity. Also for the human Tal, a decrease in activity was observed upon amino acid replacement. With 29 units/mg hTal exhibits a lower V_{max} than TalB. However, with 12 ± 2 units/mg the activity of the hTalF189Y mutein is similar to the TalB variant. So far hTal had been described to posses a specific activity ≥15 units/mg (27). The K_m values with 2.3 mM for the wild-type and 27 ± 4 mM for the hTalF189Y mutein are comparable with the corresponding *E. coli* homolog. The catalytic efficiencies of both human variants are a factor of two lower than of the corresponding TalB variant. For FSA, no increase in activity upon addition of Ery-4-P (2 mM) was observed.

Structure of the His_6-TalBF178Y Mutein—The structure of the unliganded His_6-TalBF178Y mutein was determined to 1.4-Å resolution. This is the highest resolution so far available for a transaldolase (5–7). The structures of wild-type and mutant transaldolase are very similar; superimposition of the subunit results in root mean square deviation values of 0.38 Å for 315 eq Cα atoms. Apart from the introduced amino acid replacement there are no structural changes visible in the active site (Fig. 6). We also attempted to determine the structure of the reduced Schiff base intermediate. However, we were not successful in reducing the Schiff base intermediate for the His_6-TalBF178Y mutein. A reduction of the Schiff base intermediate should have led to an inactivation of the enzyme. In contrast to the wild-type enzyme, the TalBF178Y mutein was still active after incubation with substrate and $NaBH_4$ treatment (data not shown).

DISCUSSION

Mutagenesis—Previously, the function of conserved residues in the active site of TalB was investigated using site-directed mutagenesis (4). The muteins were characterized by kinetic analysis and determination of their structure. However, Phe^{178} was not included in that study. The aim of the study presented here was to investigate whether fructose-6-phosphate aldolase activity can be evolved from TalB of *E. coli*. A possible role of Phe^{178} in this conversion was suggested by the comparison of the three-dimensional structure of TalB (5) with that of FSA (9). Instead of a total random approach and generation of a library with methods like error-prone PCR we opted to make use of the structural information available to us and generate focused libraries on selected positions. This strategy had been shown by different groups and on different enzymes to achieve the desired activity (28–33).

[4] W.-D. Fessner, personal communication.

TABLE 3
Kinetics for His_6-TalB and His_6-TalBF178Y from *E. coli*, and hTal and hTalF189Y from *H. sapiens sapiens* for the transaldolase reaction

Protein		His_6-TalBwt	His_6-TalBF178Y	FSA	hTalwt	hTalF189Y
Reaction						
Ser-7-P and GAP	V_{max} (units/mg)	85 ± 9^a	14 ± 1^b	ND[c]	29^d	12 ± 2^a
Formation from	k_{cat}[e] (s^{-1})	53 ± 6^a	8.8 ± 0.5^b	ND	18^d	7.4 ± 1.1^a
Fru-6-P and Ery-4-P	K_m (F6P) (mM)	3.0 ± 0.2^a	22 ± 5^b	ND	2.3^d	27 ± 4^a
	k_{cat}/K_m (M^{-1} s^{-1})	$(18 \pm 3) \times 10^3$	$(0.53 \pm 0.13) \times 10^3$	ND	8.0×10^3	$(0.28 \pm 0.03) \times 10^3$

[a] Average value from three independent measurements.
[b] Average value from five independent measurements.
[c] ND, not determined; activity <0.01 unit/mg (no increase in activity over Fru-6-P (10 mM) cleavage upon Ery-4-P (2 mM) addition).
[d] Average value from two independent measurements (deviation ≤15%).
[e] k_{cat} was calculated as turnover number per active sites, *i.e.* monomeric subunits.

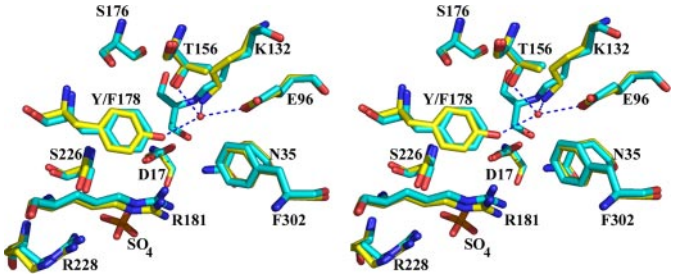

FIGURE 6. **Comparison of the x-ray structures of the active site of the TalBwt-reduced Schiff base complex (*blue*) (6) with the x-ray structure of TalBF178Y (*yellow*).** A catalytic active water molecule forms hydrogen bonds with residues Glu^{96} and Thr^{156} in the wild-type enzyme, whereas in the mutein residue Tyr^{178} is able to form a third hydrogen bound. A sulfate ion from the buffer is in close proximity to residues Arg^{181}, Ser^{226}, and Arg^{228} and indicates the binding site of the phosphate group of the substrates.

For the generation of the libraries, we used the QuikChange II Site-directed mutagenesis kit from Stratagene, which gives very high mutation rates in our hands. This was confirmed as none of the 30 randomly sequenced clones contained the wild-type codon that was not possible to regain with the degenerated primers used (replacement codon NNS). The 30 clones sequenced display 17 different codons at the position of mutagenesis. Four of the 30 clones showed an insertion of a small DNA fragment corresponding to 13% of the clones and two showed additional mutations. Another problem is the overrepresentation of the triplet TAC coding for Tyr. This codon is present in about 13% of the clones. As the degenerate codon NNS was used in the mutagenesis primers 32 codons are possible. Therefore, a single codon should be present in only 3% of the clones. Two other codons seem to be overrepresented (AAC and AGC). The reason for this overrepresentation is not clear. As the clones for sequencing were picked randomly no matter whether they show any activity or not, a bias for active clones can be ruled out. Another possible reason could be that during primer synthesis the codons were not incorporated equally and there is already a bias toward certain codons in the synthesized primer mixture. An alternative explanation could be that certain primers anneal better to the template and hence yield more PCR product than others. However, according to Georgescu *et al.* (34) a minimal library size of 72 clones is required for 90% coverage and 95 clones for 95% coverage. As 252 clones were screened there should be a good chance to cover all possible amino acid replacements.

Kinetic Properties of the TalBF178Y Mutein—The effect caused by this single replacement from a Phe to a Tyr is quite dramatic. It increased the activity of the His_6-TalB variant in the FSA reaction by 70-fold from 0.1 (wt activity) to 7 units/mg and also increases the affinity of DHA to 30 mM. This leads to an enzyme with a similar catalytic efficiency as FSA. However, the His_6-TalBF178Y mutein does not behave in all aspects similar to FSA. For example, using high pressure liquid chromatography for detection of product formation, hydroxyacetone, which was previously shown to be a donor substrate for FSA (35), is not accepted by the His_6-TalBF178Y mutein (data not shown). The activity in the direction of cleavage is considerably lower. Due to thermodynamic reasons the equilibrium for DHA and DHAP-dependent aldolases favors synthesis (26). The K_m value for Fru-6-P seems to vary depending on the type of reaction considered, Fru-6-P cleavage or Tal reaction. One should remember that the K_m value although a measure for the affinity of a substrate is not the same as the dissociation constant. But according to the model of Briggs and Haldane (36) assuming a steady-state the K_m term consists of all velocity constants for the formation and breakdown of the enzyme substrate complex. Therefore, the term varies whether a two-substrate reaction with a ping-pong mechanism (Tal reaction) is considered or a one substrate reaction (Fru-6-P cleavage).

The replacement of Ala^{247} by Thr, which is present in both His_6-TalBwt and His_6-TalBF178Y, does not alter its kinetic properties. Previously, the Tal reaction for TalBwt had been described with a V_{max} of 80 units/mg and a K_m value for Fru-6-P of 1.2 mM (1).

Role of Phe^{178}—As the structures of TalB and FSA are available and the structure of the TalBF178Y mutein was presented here it is possible to draw some conclusions about the effect of the replacement of Phe^{178} by Tyr. The replacement does not lead to unintended structural changes in the active site. Rather the difference in activity might be caused by a different chemistry in the active site. Interestingly, FSA possesses a tyrosine (Tyr^{131}) at the equivalent position to Phe^{178} of TalB. In FSA, Tyr^{131} extends into the active site and together with Gln^{59} and Thr^{109} binds a catalytically important water molecule close to the O1 oxygen atom of the carbinolamine (9). This water molecule is thought to be involved in proton transfer to and from the substrates and reaction intermediates during the formation of the Schiff base intermediate, especially the protonation of the leaving group. In TalB, Phe^{178} cannot form an H-bond with the water molecule. Hence, the catalytically important water molecule is only coordinated by 2 residues, Glu^{96} and Thr^{156} (6) (Fig. 6). This change in H-bond pattern is suggested to influence the nucleophilicity of the water molecule and hence the stability of the Schiff base intermediate. In TalB, the intermediate is sufficiently stable for the binding of the second substrate to occur, whereas in FSA the intermediate is hydrolyzed more

easily and no transfer reaction can take place. In the structure of the unliganded TalBF178Y mutein the catalytic water molecule is at the same position as in the reduced Schiff base intermediate of TalBwt. Therefore, the different coordination of the water molecule in the TalBF178Y mutein (Fig. 6) compared with TalBwt seems to destabilize the Schiff base intermediate similar to the situation in FSA. This instability is probably the reason why we were not successful in reducing the Schiff base intermediate of the TalBF178Y mutein. The DHA moiety bound to the lysine residue in the active site probably dissociates faster than the intermediate is reduced by $NaBH_4$.

Interestingly, other residues supplying an OH-group like Ser or Thr do not show FSA activity but a reduced Tal activity (His_6-TalF178S, 1.0 units/mg; His_6-TalF178T, 0.2 units/mg). A glance at the active site in the structure of TalB suggests that these side chains are too short to form an H-bond with the catalytic water molecule.

Previous studies demonstrated that the reciprocal replacement of Tyr^{131} in FSA to Phe does not have the proposed effect. The FSAY131F mutein exhibits a low expression level and is less stable to heat treatment than the wild-type enzyme (15). No FSA activity was detectable with this mutein.

Enzyme Evolution within the Tal Family—According to their sequence similarities, Tals are divided into three groups (37) plus the subfamily of small transaldolases. Surprisingly, the Tals of Gram-negative bacteria and eukaryotes (with the exception of plants) show quite high similarity, *i.e.* 71.6% similarity (56.3% identity) between TalB from *E. coli* and hTal (see supplementary data for multiple sequence alignment). Even so, as a metabolic enzyme Tal is highly conserved in its function and spread in all domains of life this does not mean that its overall sequence is highly conserved. Only 5% of human genes have orthologs in *E. coli* (Inparanoid data base (38), inparanoid.cgb.ki.se). This high similarity in sequence is also mirrored by a similar three-dimensional structure of TalB and hTal (5, 7). These findings suggest that Tal was conserved in sequence and structure during evolution from bacteria to higher mammals. Nevertheless, divergent evolution occurred within the domain of bacteria and in the branch leading to higher plants.

Interestingly, an enzyme that by sequence and structure similarity clearly resides within the subfamily of small transaldolases does not show a transaldolase activity but a fructose-6-phosphate aldolase activity (8). The results from the TalBF178Y mutein presented here suggest that during evolution FSA could have evolved from a Tal by a few mutations.

Comparison of TalB–hTal—This study shows that results from mutagenesis studies of the well investigated *E. coli* enzyme TalB can be transferred to the human transaldolase and probably to other related transaldolases. This gained more relevance as in recent years several clinical phenotypes were described for Tal-deficient individuals. In these cases Tal deficiency was linked to homozygous individuals carrying an amino acid replacement (R192H) or deletion (ΔSer^{171}) in hTal. These individuals show severe clinical phenotypes, like liver cirrhosis, cardiomyopathy, hypoglycemia, edema, and dysmorphic features (39–42). Such mutations can be studied more easily in the *E. coli* system. Furthermore, structure-function relationships can be drawn due to the wealth of available structural and mutational data for TalB (4, 6). Tal-deficient mice developed normally but exhibit male sterility due to sperm immotility that is caused by the loss of the mitochondrial transmembrane potential (43). In human and mice such mutations are apparently more severe than in *E. coli*. On one hand, human and mice possess only one gene, whereas *E. coli* contains two isoforms (TalA and TalB). On the other hand, the metabolism of *E. coli* seems to be more flexible as even a double knock-out does not lead to any obvious phenotype.[3]

Another interesting finding is the fact that the antibody against *E. coli* TalB also recognizes hTal. hTal is discussed as an autoantigen in multiple sclerosis patients. Multiple sclerosis patients display antibodies against hTal in their plasma and cerebospinal fluid. It was shown that oligodendrocytes, which form the myelin sheet, selectively express high amounts of hTal. These cells are destroyed in multiple sclerosis patients by cytotoxic T cells. It is discussed that this autoimmune reaction is caused by a cross-reactivity of antibodies originally directed against retroviral core proteins, which show small sequence stretches with high similarity to patches on the surface of hTal (44–46). Antibodies directed against these retroviral proteins show cross-reactivity to hTal and were found in multiple sclerosis patients (44–46). Our findings now suggest that antibodies that were originally directed against a protein of a microorganism could show cross-reactivity and cause an autoimmune disorder. To our knowledge, there is no report in the literature to date that this cross-reactivity could be caused by bacterial and not by viral proteins.

Acknowledgments—We are grateful to Silvia Lakner for help with cloning and strain construction. We acknowledge access to synchrotron radiation at beam line ID14-3, ESRF, France.

REFERENCES

1. Sprenger, G. A., Schörken, U., Sprenger, G., and Sahm, H. (1995) *J. Bacteriol.* **177,** 5930–5936
2. Schneider, G., and Sprenger, G. A. (2002) *Methods Enzymol.* **354,** 197–201
3. Schörken, U., Jia, J., Sahm, H., Sprenger, G. A., and Schneider, G. (1998) *FEBS Lett.* **441,** 247–250
4. Schörken, U., Thorell, S., Schürmann, M., Jia, J., Sprenger, G. A., and Schneider, G. (2001) *Eur. J. Biochem.* **268,** 2408–2415
5. Jia, J., Huang, W., Schörken, U., Sahm, H., Sprenger, G. A., Lindqvist, Y., and Schneider, G. (1996) *Structure* **4,** 715–724
6. Jia, J., Schörken, U., Lindqvist, Y., Sprenger, G. A., and Schneider, G. (1997) *Protein Sci.* **6,** 119–124
7. Thorell, S., Gergely, P., Jr., Banki, K., Perl, A., and Schneider, G. (2000) *FEBS Lett.* **475,** 205–208
8. Schürmann, M., and Sprenger, G. A. (2001) *J. Biol. Chem.* **276,** 11055–11061
9. Thorell, S., Schürmann, M., Sprenger, G. A., and Schneider, G. (2002) *J. Mol. Biol.* **319,** 161–171
10. Hayashi, K., Morooka, N., Yamamoto, Y., Fujita, K., Isono, K., Choi, S., Ohtsubo, E., Baba, T., Wanner, B. L., Mori, H., and Horiuchi, T. (2006) *Mol. Syst. Biol.* **2,** 2006 0007
11. Fürste, J. P., Pansegrau, W., Frank, R., Blöcker, H., Scholz, P., Bagdasarian, M., and Lanka, E. (1986) *Gene* (*Amst.*) **48,** 119–131
12. Sambrook, J., Fritsch, E. F., and Maniatis, T. (1989) *Molecular Cloning: A Laboratory Manual*, 2nd Ed., Cold Spring Harbor Laboratory, Cold Spring Harbor, NY
13. Bradford, M. M. (1976) *Anal. Biochem.* **72,** 248–254
14. Laemmli, U. K. (1970) *Nature* **227,** 680–685

15. Inoue, T. (2006) *Microbial Aldolases as C-C Bonding Enzymes: Investigations of Structural-Functional Characteristics and Application for Stereoselective Reactions*, Ph.D. thesis, Universität Stuttgart, Stuttgart, Germany
16. Tsolas, O., and Horecker, B. L. (1972) *The Enzymes*, 3rd Ed., Academic Press, New York
17. Collaborative Computational Project, N. (1994) *Acta Crystallogr. Sect. D Biol. Crystallogr.* **50,** 760–763
18. Vagin, A. A., and Teplyakov, A. (1997) *J. Appl. Crystallogr.* **30,** 1022–1025
19. Murshudov, G., Vagin, A. A., and Dodson, E. J. (1997) *Acta Crystallogr. Sect. D Biol. Crystallogr.* **53,** 240–253
20. Emsley, P., and Cowtan, K. (2004) *Acta Crystallogr. Sect. D Biol. Crystallogr.* **60,** 2126–2132
21. Banki, K., Halladay, D., and Perl, A. (1994) *J. Biol. Chem.* **269,** 2847–2851
22. Rosenberg, A. H., Lade, B. N., Chui, D. S., Lin, S. W., Dunn, J. J., and Studier, F. W. (1987) *Gene* (*Amst.*) **56,** 125–135
23. Novy, R., Drott, D., Yaeger, K., and Mierendorf, R. (2001) *inNovations* **12,** 1–3
24. Datsenko, K. A., and Wanner, B. L. (2000) *Proc. Natl. Acad. Sci. U. S. A.* **97,** 6640–6645
25. Parks, T. D., Howard, E. D., Wolpert, T. J., Arp, D. J., and Dougherty, W. G. (1995) *Virology* **210,** 194–201
26. Gefflaut, T., Blonski, C., Perie, J., and Willson, M. (1995) *Prog. Biophys. Mol. Biol.* **63,** 301–340
27. Banki, K., and Perl, A. (1996) *FEBS Lett.* **378,** 161–165
28. Jager, S. A., Shapovalova, I. V., Jekel, P. A., Alkema, W. B., Svedas, V. K., and Janssen, D. B. (2008) *J. Biotechnol.* **133,** 18–26
29. Amiss, T. J., Sherman, D. B., Nycz, C. M., Andaluz, S. A., and Pitner, J. B. (2007) *Protein Sci.* **16,** 2350–2359
30. Ang, E. L., Obbard, J. P., and Zhao, H. (2007) *FEBS J.* **274,** 928–939
31. Fujii, K., Minagawa, H., Terada, Y., Takaha, T., Kuriki, T., Shimada, J., and Kaneko, H. (2005) *Appl. Environ. Microbiol.* **71,** 5823–5827
32. Parikh, M. R., and Matsumura, I. (2005) *J. Mol. Biol.* **352,** 621–628
33. Williams, G. J., Woodhall, T., Nelson, A., and Berry, A. (2005) *Protein Eng. Des. Sel.* **18,** 239–246
34. Georgescu, R., Bandara, G., and Sun, L. (2003) *Directed Evolution Library Creation: Methods and Protocols*, Humana Press Inc., Totowa, NJ
35. Schürmann, M., Schürmann, M., and Sprenger, G. (2002) *J. Mol. Catal. B Enzym.* **19–20,** 247–252
36. Briggs, G. E., and Haldane, J. B. (1925) *Biochem. J.* **19,** 338–339
37. Kohler, U., Cerff, R., and Brinkmann, H. (1996) *Plant Mol. Biol.* **30,** 213–218
38. Remm, M., Storm, C. E., and Sonnhammer, E. L. (2001) *J. Mol. Biol.* **314,** 1041–1052
39. Valayannopoulos, V., Verhoeven, N. M., Mention, K., Salomons, G. S., Sommelet, D., Gonzales, M., Touati, G., de Lonlay, P., Jakobs, C., and Saudubray, J. M. (2006) *J. Pediatr.* **149,** 713–717
40. Verhoeven, N. M., Huck, J. H., Roos, B., Struys, E. A., Salomons, G. S., Douwes, A. C., van der Knaap, M. S., and Jakobs, C. (2001) *Am. J. Hum. Genet.* **68,** 1086–1092
41. Verhoeven, N. M., Wallot, M., Huck, J. H., Dirsch, O., Ballauf, A., Neudorf, U., Salomons, G. S., van der Knaap, M. S., Voit, T., and Jakobs, C. (2005) *J. Inherit. Metab. Dis.* **28,** 169–179
42. Grossman, C. E., Niland, B., Stancato, C., Verhoeven, N. M., Van Der Knaap, M. S., Jakobs, C., Brown, L. M., Vajda, S., Banki, K., and Perl, A. (2004) *Biochem. J.* **382,** 725–731
43. Perl, A., Qian, Y., Chohan, K. R., Shirley, C. R., Amidon, W., Banerjee, S., Middleton, F. A., Conkrite, K. L., Barcza, M., Gonchoroff, N., Suarez, S. S., and Banki, K. (2006) *Proc. Natl. Acad. Sci. U. S. A.* **103,** 14813–14818
44. Banki, K., Colombo, E., Sia, F., Halladay, D., Mattson, D. H., Tatum, A. H., Massa, P. T., Phillips, P. E., and Perl, A. (1994) *J. Exp. Med.* **180,** 1649–1663
45. Esposito, M., Venkatesh, V., Otvos, L., Weng, Z., Vajda, S., Banki, K., and Perl, A. (1999) *J. Immunol.* **163,** 4027–4032
46. Schmidt, S. (1999) *Mult. Scler.* **5,** 147–160